

Assembly of Gold Nanoparticles on Electrospun Polymer Nanofiber Film for SERS Applications

Li Wang,* Yujing Sun,[†] Jiku Wang, and Zhuang Li[†]

*College of Chemistry, Jilin Normal University, Siping 136000, P.R. China. *E-mail: liwang_jlnu@163.com*

[†]State Key Laboratory of Electroanalytical Chemistry, Changchun Institute of Applied Chemistry,

Chinese Academy of Sciences, Changchun 130022, P.R. China

Received August 29, 2013, Accepted October 2, 2013

We report a novel approach for fabricating active surface-enhanced Raman scattering (SERS) substrate for sensitive detection. This approach is based on the assembling of gold nanoparticles (AuNPs) onto the electrospun polycaprolactone (PCL) nanofiber film. The hydrophobic surface of PCL nanofiber film was pretreated using UV-inducing graft polymerization with acrylic acid. Afterwards this PCL nanofiber film was incubated with the AuNP solution to promote the assembly of AuNPs onto the PCL nanofibers and the formation of SERS active substrate. 4-aminothiophenol (4-ATP) molecule was used as a test probe for SERS experiments, indicating that the substrate has high sensitivity to SERS response. Our method has great advantage in term of environment-friendly synthesis, large-scale, high stability and good reproducibility. This highly active SERS substrate can be employed to detect the drug molecule, 2-thiouracil.

Key Words : PCL, Gold, Nanoparticle, SERS, 2-Thiouracil

Introduction

Surface-enhanced Raman scattering (SERS) spectroscopy is a very powerful tool to study the molecule/metal nanoparticle system, due to its abundant molecular structure information, high sensitivity, and surface selectivity.^{1,2} This ultrasensitive analytical method has been widely applied on the life and environmental science,^{3,4} which inspire a worldwide effort to explore its mechanism both theoretically and experimentally. Various substrates with rough surface were developed for SERS study, such as metallic colloids,^{5,6} electrochemically roughened electrodes,^{7,8} chemically deposited metal films,^{9,10} chemically etched metal nanostructures,¹¹ and so on. Among these substrates, colloidal gold (Au) and silver (Ag) nanoparticles (NPs) have been widely used because of their easy preparation and strong enhancement for the SERS detection. Importantly, gold and silver colloids as substrates offer a tremendous enhancement of the intensity of the vibrational signals over 10 orders of magnitude. For the past few years, various techniques have been used for controllable assembly of Au or Ag NPs into specific structures with SERS activity. Electron beam lithography,¹² template method,¹³ and interface assembly¹⁴ *etc.* are currently available avenue for the fabrication of well ordered, periodic Au and Ag NP arrays with desired morphology. However, these techniques either require multiple steps or are hard to extend to large scales for routine SERS detection, which limit their practical applications. Therefore, some new strategies are needed to prepare SERS-active substrates with good stability, easy and reproducible preparation, low cost and high sensitivity.

Polycaprolactone (PCL), a biodegradable aliphatic polyester, has been employed as a bioresorbable polymer in the

medical devices and for tissue engineering applications owing to its biocompatibility and slow degradation rate.^{15,16}

In this paper, we presented a novel strategy to fabricate highly sensitive, reproducible, stable, large-scale, and reliable SERS substrate by the assembly of AuNPs onto the electrospun PCL nanofiber film. Because the surface of PCL nanofiber is hydrophobic, the PCL nanofiber film was first modified by grafting copolymerization of acrylic acid initiated under UV light. This hydrophilized nanofiber film was incubated in the freshly prepared AuNP solution for the controllable assembly of AuNPs onto the PCL nanofibers. The optimal SERS-active substrate could be prepared by systematically adjusting the experimental parameters, including the layer number of PCL nanofibers and the incubation time of PCL nanofiber film in the AuNP solution. The SERS substrates prepared by our method show excellent enhancement ability, and can be employed to detect 2-thiouracil (2-TU).

Experimental

Chemicals and Materials. PCL ($M_w=80,000$) was purchased from Alfa Aesar. Acrylic acid and Vitamin B2 were purchased from J&K Scientific Ltd. Hydrogen tetrachloroaurate tetrahydrate ($\text{HAuCl}_4 \cdot 4\text{H}_2\text{O}$, A. R.), sodium borohydride (A. R.) and ethanol (G. R.) were supplied by Beijing chemical Reagent Co. 2-thiouracil (2-TU) was purchased from TCI (Shanghai) Development Co., Ltd. 4-aminothiophenol (4-ATP) and cysteine were obtained from Alfa Aesar. All chemicals were used without further purification. The water used throughout the experiments was ultrapure water.

Preparation of SERS Substrates. PCL nanofiber films were prepared according to the literature protocols.¹⁷ PCL

was dissolved in a mixture of ethanol and water (40:60, v/v), and then loaded into a plastic syringe of 10 mL with a 20 gauge blunt tip needle and were dispensed at a rate of 0.1–0.3 mL·h⁻¹ during the electrospinning. The biaxially oriented nanofiber films were prepared by electrospinning multiple layers in the direction of 0° and 90° alternately. The first layer of nanofiber could be electrospun onto aluminium foil that attached to the collector, and the second layer on the top of the first one could be obtained by rotating the aluminium foil for 90°, and the spraying time was 10 min for each layer of fibers. Then repeated the above procedure until getting desired PCL nanofiber films. All the samples were electrospun with an applied voltage of 7–9 kV at a distance of 15 cm from the needle tip to the rotating drum. The obtained film was cut into square pieces in 1.0 × 1.0 cm² dimensions. For hydrophilizing PCL nanofiber surface, 50 µL aqueous solution containing 1.2 M acrylic acid and 0.7 mM Vitamin B2 was dropped onto these PCL pieces, respectively. After that, the pieces were clipped between two quartzes, and then exposed to UV illumination for 30 min. After graft polymerization, the pieces were removed from the reaction set and washed with water.

For preparing AuNPs, 412 µL of 48.6 mM aqueous HAuCl₄ was diluted to 20 mL with water, and then 1 mL of 1 mM aqueous cysteine was added into this solution. Under vigorous stirring, 250 µL of 0.5% NaBH₄ aqueous solution was dropped into the mixed solution. The solution turned amaranth in color, showing the formation of AuNPs. The hydrophilized PCL pieces were incubated in the AuNP solution for 30, 60 and 120 min, respectively. After that, the pieces were washed with water, and dried in air. Then, they were used for characterizations and SERS tests.

Characterization. Scanning electron microscopy (SEM) and X-ray energy dispersive spectroscopy (EDS) characterizations were carried out on an XL30 ESEM FEG field emission scanning electron microscopy (FEI Company) with an accelerating voltage of 20 kV. The Raman spectra were obtained with a FT-Raman spectrometer (Thermo Nicolet 960) equipped with an InGaAs detector and Nd/VO₄ laser (1064 nm) as an excitation source. The laser power was about 0.3 W. The number of sample scans is 1024, and the resolution is 8 for all the measurements.

Results and Discussion

Preparation of PCL and AuNPs-based Substrates. The PCL pieces before and after incubation in the AuNP solution were characterized by SEM and EDS, as shown in Figure 1. The PCL nanofiber film is composed of hundreds of micrometer fibers in length. Almost all of the nanofibers are straight and their surface is smooth (Figure 1(a)). The fibers alternately arrange in three-dimensional (3-D) space. After the PCL piece was incubated in the AuNP solution for 30 min, the AuNPs were assembled onto the surface of PCL fibers (Figure 1(b)). The AuNPs with an average diameter of about 73 nm were in a state of aggregation, and the aggregations dispersed on the PCL nanofibers. It is worth noting

that the AuNPs were only adsorbed onto the surface of PCL nanofibers, whereas the AuNPs were not observed outside the PCL fibers. These suggest that the hydrophilization process of the PCL nanofiber film was successful, thus the AuNPs capped by cysteine could be assembled onto the PCL nanofibers through electrostatic interaction. The AuNPs stabilized by cysteine, a bifunctional molecule, tend to connect each other by intermolecular hydrogen bondings.¹⁸ Therefore, only the NP aggregations can be observed on the PCL fibers, and the monodispersed particles can't be found. When the incubation time was 60 min, it can be clearly seen from Figure 1(c) that more AuNPs were adsorbed onto the PCL nanofibers compared to that with 30 min incubation (Figure 1(b)). As the incubation time was increased to 120 min, a great deal of AuNPs was assembled onto the PCL nanofibers, to form more and bigger NP aggregations (Figure 1(d)). Figure 1(e) gives the EDS analysis of the product, confirming the presence of metal Au. From Figure 1(b) and 1(c), it can be seen that the resultant nanostructures are 3-D due to the 3-D architecture of PCL nanofiber film. With the elongation of incubation time, more AuNPs were adsorbed onto the PCL fibers, resulting in the weakening of this kind of 3-D structure as shown in Figure 1(d).

The PCL pieces after incubated in the AuNP solution can serve as SERS substrates for molecular sensing with high sensitivity and specificity. In our work, 4-ATP was chosen as a probe molecule to evaluate the ability of SERS enhancement of the substrates. Simply, 20 µL of 1 × 10⁻⁵ M 4-

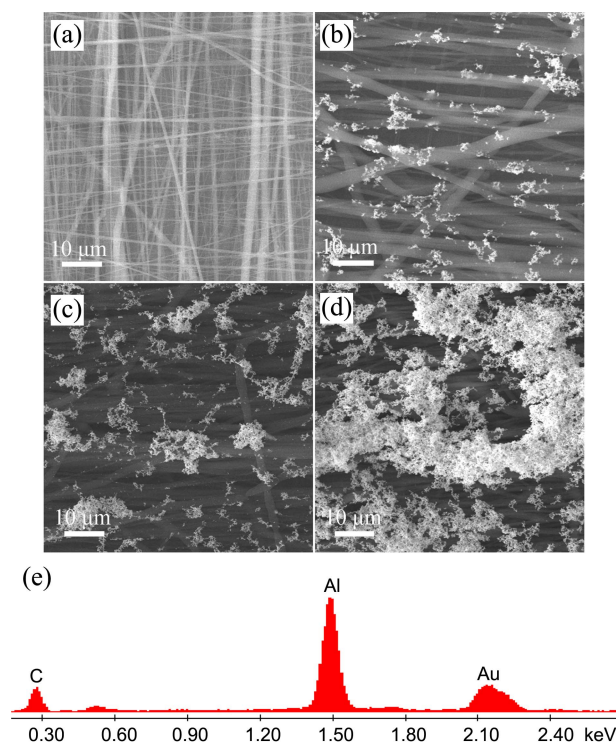


Figure 1. SEM images of the PCL pieces before (a) and after (b, c, d) incubation in the AuNP solution. The incubation time is (b) 30 min, (c) 60 min, and (d) 120 min, respectively. (e) EDS characterization of the PCL piece after incubated in the AuNP solution for 120 min.

ATP ethanol solution was dropped onto the sample surface, and then dried in air. Figure 2(a) depicts a set of FT-SERS spectra of 4-ATP on the various substrates. For comparison, the normal FT-Raman spectrum of solid 4-ATP was shown in Figure 2(b). The obvious difference between the two spectra is frequency shifts and some changes in the intensity for most of the bands. For example, the $\nu(\text{CS})$ band shifts from 1086 cm^{-1} in Figure 2(b) to 1078 cm^{-1} in Figure 2(a), and $\nu(\text{CC})$ band shifts from 1591 to 1587 cm^{-1} . These changes in several main bands imply that the $-\text{SH}$ group in 4-ATP directly contacts with the AuNP surface.¹⁹ The band at 465 cm^{-1} in Figure 2(b) is missing, and a new band at 391 cm^{-1} appears in Figure 2(a) corresponds to one of the vibration modes of C–S bond, most likely the bending mode of C–S bond.^{20,21} The predominant bands in the SERS spectra are located at 1587 and 1078 cm^{-1} , which belong to the a_1 vibration modes. The apparent enhancement *via* an electromagnetic (EM) mechanism is significant.²² In addition, the b_2 modes located at 1178 and 1005 cm^{-1} can also be observed. The enhancement of b_2 modes has been ascribed to the charge transfer (CT) of the metal to the adsorbed molecules, which indicates 4-ATP contact with Au nanostructure surface by forming a strong Au–S bond.^{19,20,23} The intensity of the SERS signal is different for each of the PCL pieces that incubation in the AuNP solution for different periods. When the incubation time ranged from 30 to 60 min, the obtained PCL pieces as substrates have relatively large SERS signal (shown in Figure 2(a) and 2(b)). As the incubation time continued increasing, the SERS activity of the substrate became weaker and weaker (Figure 2(c)). The reason of difference in the enhancement effect may be that, the assemblies/aggregation of particles could favor the formation of massive localized plasmon excitations, namely hot-spots that is believed to be responsible for producing the huge amplifications in single molecule SERS.^{24,25} However, when the incubation time was increased, more NP aggregations adsorbed onto the PCL fibers (Figure 1(d)), resulting in the decrease of hot-spots. The large aggregates formed precipitate, which decreases the interparticle distance and causes the decrease of hot-spots and SERS enhancement. Additionally, because the cysteine-capped NPs had a strong trend to aggregate in solution, the longer the incubation time was, the closer the NPs inter-connected, and the more NP aggregations adsorbed on the PCL fibers was, which weakened 3-D structure characteristic of the substrate. In these spectra, the intensities for some interference peaks are increasing along the incubation time. The origin for those interferences could be coming from the increase of cysteine concentration.

The surface enhancement factor (EF) of 4-ATP on the substrate was calculated according to the following equation:

$$\text{EF} = (I_{\text{SERS}}/I_{\text{Raman}}) \times (M_{\text{bulk}}/M_{\text{surface}})$$

where I_{SERS} and I_{Raman} stand for the intensities of a vibrational mode in the SERS and normal Raman spectrum of 4-ATP, respectively; M_{bulk} is the molecule number of the neat

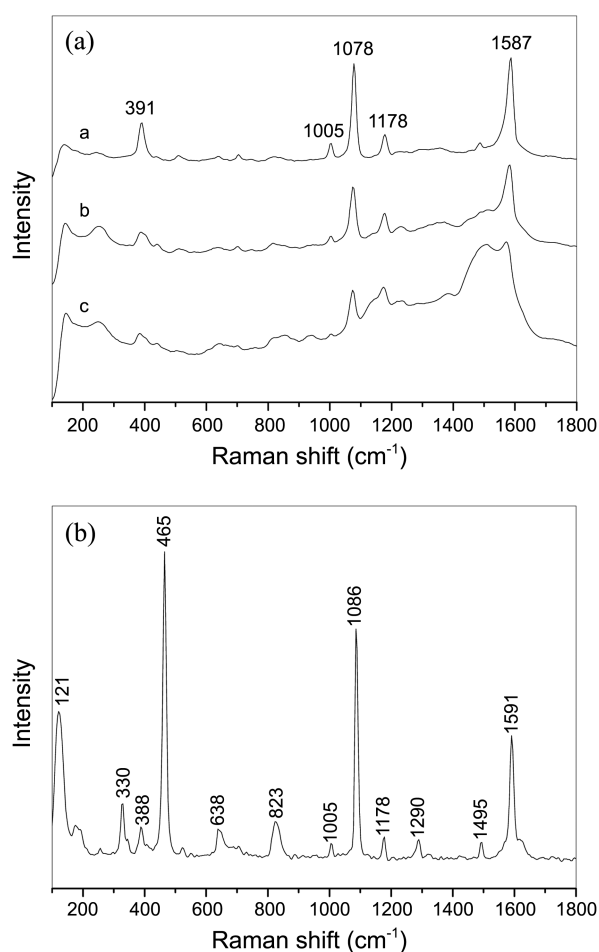


Figure 2. (A) FT-SERS spectra of 4-ATP (1×10^{-5}) on the PCL pieces that incubation in the AuNP solution for different time: (a) 30 min, (b) 60 min and (c) 120 min. (B) The normal FT-Raman spectra of solid 4-ATP.

4-ATP in the laser illumination volume; and M_{surface} is the number of molecules adsorbed and sampled on the SERS active substrate within the laser spot. In the sample area ($\sim 100\text{ }\mu\text{m}$ in diameter) measured, M_{surface} was calculated to be 9.5×10^9 . Taking the laser spot ($\sim 100\text{ }\mu\text{m}$ in diameter), the penetration depth (about $\sim 180\text{ }\mu\text{m}$) and the density of 4-ATP ($1.17\text{ g}\cdot\text{mL}^{-1}$) into account,²⁶ The value of M_{bulk} was 7.9×10^{15} in the detected solid sample area. For the vibrational modes at 1591 cm^{-1} (ν_{CC}), the EF was estimated to be about 3.7×10^6 . We suggest that the formation of the SERS effect on these substrates is the result of the synergistic effect of CT and EM mechanism, namely that the combination of chemical and physical enhancement mechanism. The advantages of the PCL pieces modified by the AuNPs as SERS substrates are three folds. First, it has relatively large surface area for anchoring many probe molecules, resulting in great enhancement. Second, the abundant inter-NP junctions can provide a huge electromagnetic field to enhance the Raman Signal.²⁷ More importantly, the special 3-D nanostructures make the substrate having much larger surface area and more hot-spots, favoring the improvement of the SERS activity.¹⁴

It worth noting that the laser selected in this work plays an important role in this SERS enhancement. Previously, Duyne *et al.* reported that the laser wavelength plays a key role in the EF value.²⁸ It was found that the SERS EF value is optimized when the energy of the localized surface plasmon resonance (LSPR) lies between the energy of the excitation wavelength and the energy of the vibrational band of interest. Therefore, in this work, we use the off-surface plasmon resonance condition (1064 excitation), which is far away from the surface plasmon resonance (SPR) of the Au NPs of any shape. At this excitation source, the surface plasmon excitation has a small contribution to the observed enhanced Raman scattering process. This strategy is favorable to demonstrate the SERS activity of these gold nanostructures.

The influence of the layer number of PCL nanofibers on the SERS activity of the prepared substrates was investigated. Figure 3 exhibits the FT-SERS spectra of 4-ATP on the SERS substrates prepared by assembling AuNPs onto the PCL pieces with different layer number of nanofibers. It can be observed that the incubated PCL piece consisting of 2-layer nanofibers as substrate has relative weak SERS enhancement ability (Figure 3(a)). The SERS signal of the substrates with 4- and 6-layer PCL nanofibers are similar (Figure 3(b) and 3(c)), but significantly stronger than that of the substrate with 2 layers of nanofibers. For example, the quantitative comparison of the peak intensity at 1078 cm^{-1} (C-S vibration) indicates that the SERS enhancements on 4- and 6-layer nanofiber substrates are approximately 1.67- and 1.75-folds of that on 2-layer nanofiber substrate. With the increase of the layer number of nanofibers, the 3-D characteristic of PCL nanofiber film became obvious, and more AuNPs were adsorbed onto the PCL nanofiber substrates. These caused the 3-D structure characteristic of the incubated PCL pieces more evident, and the pieces as SERS-active substrates have good enhancement ability.

The PCL pieces after incubated in the AuNP solution as substrates can be employed to detect biologically important

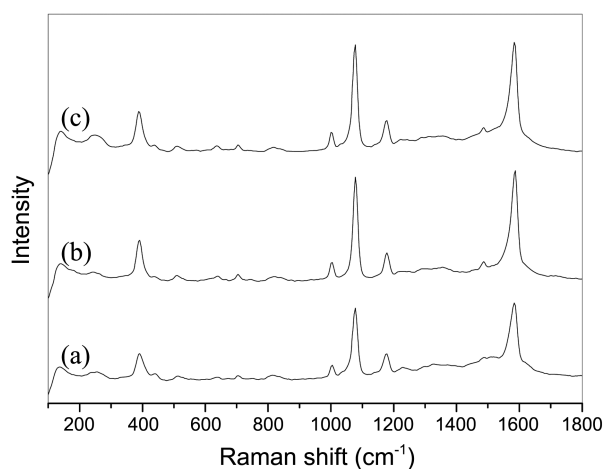


Figure 3. FT-SERS spectra of 4-ATP on the SERS substrates prepared by assembling AuNPs onto the PCL pieces with different layer number of nanofibers: (a) 2 layers, (b) 4 layers and (c) 6 layers.

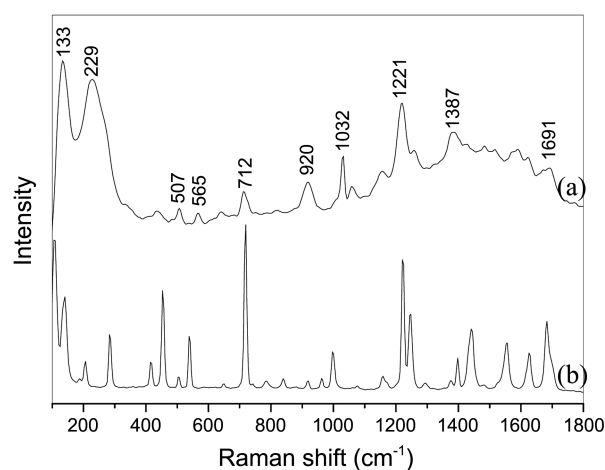


Figure 4. (a) FT-Raman spectra of 2-TU (1×10^{-5} M) on the SERS-active substrate, (b) the normal FT-Raman spectrum of solid 2-TU.

2-TU molecule. 2-TU and its derivatives show high anti-thyroid, antiviral, and antitumor activity.²⁹ Sensitive detection of 2-TU at low concentration is important for pharmacokinetic and clinical studies. 20 μL of 1×10^{-5} M 2-TU ethanol solution was casting onto the prepared SERS substrate, and then dried in air. Figure 4(a) gives the FT-SERS spectrum of 2-TU on the SERS substrate. The spectrum agrees with the previous report.³⁰ The 2-TU (1×10^{-5} M) can not be measured in the absence of SERS-active substrate, and the normal Raman spectrum of solid 2-TU was shown in Figure 4(b) to confirm the enhancement effect. Relative to the normal FT-Raman spectrum, the apparent differences in the FT-SERS spectrum include frequency shift and some changes on the intensity for the bands. It should be noted that different enhancements were obtained for different vibration peaks in this part of experiment, and it is not suitable to calculate the EF to 2-TU molecules, but it is clear that our SERS-active substrate reveals proper enhancement on detecting low-concentrated small molecules. For example, the band located at 920 cm^{-1} corresponding to the in plane bending of N(3)CC and ring is obviously enhanced (approximate 6-folds). The result indicates that the substrates prepared by our method are high-active and effective for the ultrasensitive detection of different analytes.

Conclusion

In conclusion, a facile and effect strategy was provided to prepare ultrasensitive SERS-active substrates. After the PCL nanofiber films were hydrophilically modified, they were incubated in the AuNP solution, and the cysteine-capped AuNPs were assembled onto the PCL nanofibers by electrostatic interaction. The incubated PCL pieces as substrates show excellent SERS activity, and they could be used to detect 4-ATP and 2-TU with very low concentration and high sensitivity. This work demonstrated that the substrates fabricated by our method are potential for practical detection applications.

Acknowledgments. This work was financial supported by the Jilin Province Science and Technology Development Foundation of China under Grant No. 20120577, the Science and Technology Research Program of Education Bureau of Jilin Province (Grant No. 2011165) and the National Nature Science Foundation of China (Grant No. 21077041). And the publication cost of this paper was supported by the Korean Chemical Society.

References

1. Kneipp, K.; Kneipp, H.; Itzkan, I.; Dasari, R. R.; Feld, M. S. *Chem. Rev.* **1999**, *99*, 2957.
2. Zhou, Q.; Fan, Q.; Zhuang, Y.; Li, Y.; Zhao, G.; Zheng, J. *J. Phys. Chem. B* **2006**, *110*, 12029.
3. Jarvis, R. M.; Goodacre, R. *Chem. Soc. Rev.* **2008**, *37*, 931.
4. Gunawidjaja, R.; Peleshanko, S.; Ko, H.; Tsukruk, V. V. *Adv. Mater.* **2008**, *20*, 1544.
5. Creighton, J. A.; Blatchford, C. G.; Albrecht, M. G. *J. Chem. Soc. Faraday Trans.* **1979**, *75*, 790.
6. Leopold, N.; Lendl, B. *J. Phys. Chem. B* **2003**, *107*, 5723.
7. Ren, B.; Lin, X.; Yan, J.; Mao, B.; Tian, Z. *J. Phys. Chem. B* **2003**, *107*, 899.
8. Cao, P.; Yao, J.; Ren, B.; Mao, B.; Gu, R.; Tian, Z. *Chem. Phys. Lett.* **2000**, *316*, 1.
9. Wu, Y.; Zhao, B.; Xu, W.; Li, B.; Jung, Y. M.; Ozaki, Y. *Langmuir* **1999**, *15*, 4625.
10. Anderson, D. J.; Moskovits, M. *J. Phys. Chem. B* **2006**, *110*, 13722.
11. Lu, L.; Eychmüller, A.; Kobayashi, A.; Hirano, Y.; Yoshida, K.; Kikkawa, Y.; Tawa, K.; Ozaki, Y. *Langmuir* **2006**, *22*, 2605.
12. Abu Hatab, N. A.; Oran, J. M.; Sepaniak, M. J. *ACS Nano* **2008**, *2*, 377.
13. Peng, C.; Song, Y.; Wei, G.; Zhang, W.; Li, Z.; Dong, W. F. *J. Colloid Interf. Sci.* **2008**, *317*, 183.
14. Wang, L.; Sun, Y.; Che, G.; Li, Z. *Appl. Surf. Sci.* **2011**, *257*, 7150.
15. Cheng, Z.; Teoh, S. *Biomaterials* **2004**, *25*, 1991.
16. Zhu, Y.; Gao, C.; Shen, J. *Biomaterials* **2002**, *23*, 4889.
17. Su, Z.; Li, J.; Li, Q.; Ni, T.; Wei, G. *Carbon* **2012**, *50*, 5606.
18. Thomas, K. G.; Barazzouk, S.; Ipe, B. I.; Joseph, S. T.; Kamat, P. V. *J. Phys. Chem. B* **2004**, *108*, 13066.
19. Wang, T.; Hu, X.; Dong, S. *J. Phys. Chem. B* **2006**, *110*, 16930.
20. Zheng, J.; Li, X.; Gu, R.; Lu, T. *J. Phys. Chem. B* **2002**, *106*, 1019.
21. Criffith, W. P.; Koh, T. Y. *Spectrochim. Acta A* **1995**, *51*, 253.
22. Zheng, J.; Zhou, Y.; Li, X.; Ji, Y.; Lu, T.; Gu, R. *Langmuir* **2003**, *19*, 632.
23. Osawa, M.; Matsuda, N.; Yoshll, K.; Uchida, I. *J. Phys. Chem.* **1994**, *98*, 12702.
24. dos Santos, D. S.; Alvarez-Puebla, R. A., Jr.; Oliveira, O. N.; Arcoca, R. F., Jr. *J. Mater. Chem.* **2005**, *15*, 3045.
25. Nie, S.; Emory, S. R. *Science* **1997**, *275*, 1102.
26. Sun, L.; Zhao, D.; Zhang, Z.; Li, B.; Shen, D. *J. Mater. Chem.* **2011**, *21*, 9674.
27. Sun, Y.; Wei, G.; Song, Y.; Wang, L.; Sun, L.; Guo, C.; Yang, T.; Li, Z. *Nanotechnology* **2008**, *19*, 115604 (8pp).
28. Haynes C. L.; Yonzon, C. R.; Zhang, X.; Van Duyne, R. P. *J. Raman Spectroscopy* **2005**, *36*, 471.
29. Lindsay, R. H.; Romine, C. J.; Wong, M. Y. *Arch. Biochem. Biophys.* **1968**, *126*, 812.
30. Jena, B. K.; Raj, C. R. *Chem. Mater.* **2008**, *20*, 3546.